Published March 13, 2015

Chemical and Morphological Distinctions between Vertical and Lateral Podzolization at Hubbard Brook

Rebecca R. Bourgault*
Dep. of Plant and Soil Science
Univ. of Vermont
63 Carrigan Dr.
Burlington, VT 05405

Currently at:
Biology Dep.
Sacred Heart Univ.
5151 Park Avenue
Fairfield, CT 06825

Donald S. Ross
Dep. of Plant and Soil Science
Univ. of Vermont
63 Carrigan Dr.
Burlington, VT 05405

Scott W. Bailey
U.S. Forest Service
234 Mirror Lake Rd.
North Woodstock, NH 03262

Classical podzolization studies assumed vertical percolation and pedon-scale horizon development. However, hillslope-scale lateral podzolization also occurs where lateral subsurface water flux predominates. In this hydropedologic study, 99 podzols were observed in Watershed 3, Hubbard Brook Experimental Forest, New Hampshire. Soil horizon samples were extracted with citrate–dithionite (d) and acid ammonium oxalate (o) to quantify Fe_d, Mn_d, Al_o, and Fe_o. Optical density of oxalate extract (ODOE) was measured to assess spodic C. Amorphous organometallic complexes (AOC) were observed in thin section, for which Al, Fe, Mn, and C were quantified using scanning electron microscopy–energy dispersive X-ray spectroscopy. Porosity and AOC/mineral ratio were calculated for thin section images using ImageJ. Laterally developed spodic horizons were twice as thick as vertically developed spodic horizons and contained higher concentrations of Al and Mn but lower Fe and C. Vertically developed spodic horizons had crumb microstructure with higher porosity, while laterally developed spodic horizons were more infilled. Aluminum + 0.5Fe and ODOE in the surface of laterally developed podzols were high and lacked contrast with the spodic horizon, making Spodosol classification problematic. Vertically developed spodic horizons form by solutional translocation and precipitation of AOC under unsaturated conditions. However, laterally developed spodic horizons could form via lateral translocation of solutes or physical transport and deposition of colloidal AOC with unsaturated or saturated flow. This study demonstrates the importance of lateral podzolization in producing soils with distinctive morphology, composition, and classification. Future studies or mapping efforts in podzolized catchments should incorporate these different pedogenic processes.

Abbreviations: AOC, amorphous organometallic complexes; HPU, hydropedologic unit; LBh, laterally developed Bh horizon; LBhs, laterally developed Bhs horizon; ODOE, optical density of oxalate extract; OM, organic matter; SEM-EDS, scanning electron microscopy–energy dispersive X-ray spectroscopy; VBhs, vertically developed Bhs horizon; VBs, vertically developed Bs horizon; WS3, Watershed 3.

Podzolization is the pedogenic process leading to the formation of podzols, which are soils that contain amorphous organometallic complexes (AOC) in the B horizon. Spodic materials are mineral soil materials containing AOC and are a mixture of illuvial organic matter (OM) and Al, with or without Fe. In the USDA soil taxonomy, spodic materials have technically defined morphological and chemical characteristics, including dark and/or red colors, low pH, and high organic C. Podzols are commonly found in humid temperate climates with acidic, coarse-textured parent materials under mixed or coniferous forests. If spodic materials have precipitated to a sufficient extent, a podzol may be classified as a Spodosol in the USDA soil taxonomy. In general, spodic horizons are defined as an illuvial layer with 85% or more of the horizon consisting of spodic materi-

Soil Sci. Soc. Am. J. 79:428–439
doi:10.2136/sssaj2014.05.0190
Received 8 May 2014.
Accepted 6 Oct. 2014
*Corresponding author (bourgaultr@sacredheart.edu).

als that have a color indicating accumulation of AOC. There are two subhorizon designations for spodic horizons: h and s. The *h* indicates illuvial humus, and the *s* indicates illuvial sesquioxides (secondary Fe and Al oxides). In many cases, a soil in a temperate climate must contain a spodic horizon >10 cm thick within 200 cm of the surface to be classified as a Spodosol (Soil Survey Staff, 2010).

The most widely accepted theory of podzolization involves three interrelated steps: (i) formation of a soluble Al–Fe–organic matter complex in the soil surface; (ii) translocation of the complex with soil water; and (iii) precipitation of the complex in the B horizon (Lundstrom et al., 2000; McKeague et al., 1983). Evidence for this hypothesis can be found in several decades of podzol research, in which Al and Fe have been shown to react with OM, and their distributions are closely related in podzol profiles. For example, soluble Al in eluvial horizons of podzols is 80% organically bound (Dahlgren and Ugolini, 1989; Bishop et al., 1993). There is much evidence for complexing of Al and Fe with organic acids. These acids promote mineral weathering (Drever and Stillings, 1997), releasing more Al and Fe to participate in podzolization. Soluble organometallic complexes move with soil water, illuviating and complexing more Al and Fe as they come into contact with soil mineral surfaces in a process called *cheluviation* (Fanning and Fanning, 1989). As the soluble organometallic complexes become increasingly loaded with Al and Fe, the solubility of the complex decreases, and eventually it precipitates as AOC in the B horizon. The solubility of the complex is also decreased by increasing pH downward in the soil profile. In addition, a complex with a low ratio of metals to organic compounds may be adsorbed by already precipitated AOC (McKeague et al., 1983). The depth at which AOC precipitate in the soil profile is determined by at least two important factors. First, the mineralogy of the soil parent material affects the quantity of Fe available for complexation; if there is a large supply of Fe, the organometallic complex will quickly become saturated and will precipitate closer to the soil surface. Second, the physical stability of the soil affects the depth and lateral continuity of spodic horizons; soils experiencing pedoturbation by flora or fauna tend to have shallower, less continuous horizonation (Fanning and Fanning, 1989).

Soil scientists tend to focus on pedon-scale studies of pedogenesis, and therefore the current pedogenic theories and classification systems of podzols and Spodosols (as in other soil orders) rely on the assumption of vertical development. However, there is increasing evidence that podzolization occurs laterally along hillslopes as well as vertically within single pedons (Bailey et al., 2014; Jankowski, 2014; Sommer et al., 2000, 2001; Bardy et al., 2008; Lucas et al., 2012; Buurman et al., 2013). Sommer et al. (2001) described lateral podzolization in a sandstone catchment in the Black Forest of Germany. They found that podzol morphology varied predictably with landscape position: thick E horizons with thin spodic B horizons were found in upslope eluvial zones, while thin E horizons with thick spodic B horizons were found in downslope illuvial zones. They described lateral podzolization as a three-step process: (i) upslope mobilization of Fe, Al, and Mn; (ii) translocation with lateral flow; and (iii) immobilization (precipitation) of AOC downslope facilitated by an increase in Fe and base cations downslope. Lateral podzolization was also observed in a sandy, forested area of Poland (Jankowski, 2014). Soils found in closed depressions of glaciofluvial inland dune fields contained thick accumulations of spodic materials (Al, Fe, Mn, and OM) but did not show any evidence of eluviation from the upper part of the profile. It was deduced that lateral translocation of OM complexed with Fe and Al from the surrounding hillslopes was responsible for the observed morphology.

In a study of Watershed 3 (WS3) at Hubbard Brook Experimental Forest, New Hampshire, Bailey et al. (2014) divided the podzols of the catchment into five distinct functional soil groups. All functional groups appeared to share similar soil-forming factors except for differences in subsurface water dynamics, which produced observable differences in soil morphology. These functional groups were later identified as hydropedologic units (HPUs), defined as a system of grouping soils where local differences in water movement are more important than other soil-forming factors (Gannon, 2014). In WS3, four of the five HPUs appeared to be developed by lateral podzolization. The HPU system was not dependent on the USDA soil taxonomy and allowed grouping of soils with similar morphology and chemistry that resulted from similar hydrologic, topographic, and subsurface factors. The HPU system was not intended to replace the USDA soil taxonomy, but rather to enhance it by grouping similar soils at a finer scale useful to ecological and biogeochemical interpretations. Of the HPUs, typical podzols were the most common, found on shoulders and backslopes, and these soils showed a sequence of horizons characteristic of vertical podzolization: a thin, irregular E horizon over a thin Bhs and a relatively thicker Bs. At locations with shallow bedrock (often near the watershed divide but also at lower elevations), soils with thick E horizons were found just a few meters upslope of soils with thick Bhs horizons. These soils were morphologically similar to the E-Spodosol and Bs-Spodosol endmembers suggested by Sommer et al. (2001) to be the result of lateral podzolization. Two HPUs were designated in this zone: Bhs-podzols had thick Bhs horizons that were suggested to contain AOC leached and translocated by laterally flowing water from E-podzols upslope. In near-stream and bench areas, the soils appeared to be dominated by lateral deposition of AOC due to a decrease in slope. These soils were called Bh-podzols because they had thick, dark Bh horizons comprising most of the solum. Bimodal podzols occurred in transitional zones between typical and Bh-podzols. These had a typical sequence of horizons in the upper part but an anomalous Bh horizon in the lower part that was thought to contain laterally deposited AOC. Bailey et al. (2014) used groundwater monitoring data to show water table fluctuations within the solum of HPU's hypothesized to be influenced by lateral flow processes, which were distinctly different in each HPU. This contrasted with minimal water table incursion in the solum of typical podzols formed by vertical processes under a hydrologic regime of vertical percolation.

Previous studies of lateral podzolization have not thoroughly compared the properties and pedogenesis of vertically vs. laterally developed spodic horizons. In addition, issues with classifying laterally developed soils using the USDA soil taxonomy have not yet been addressed. Therefore, the objectives of this hydropedologic study of Watershed 3 were: (i) to compare morphological, micromorphological, and chemical properties of vertically vs. laterally developed spodic horizons; (ii) to determine differences in classification between vertically developed and laterally developed podzols using the USDA soil taxonomy; and (iii) to explore differences in pedogenesis between vertically and laterally developed podzols.

MATERIALS AND METHODS

Site Description

The study area was Watershed 3 (WS3) of Hubbard Brook Experimental Forest, New Hampshire. The site was described in detail by Likens and Bormann (1995), with further details by Bailey et al. (2014). Watershed 3 is a hydrologic reference catchment and has not been subject to experimentation aside from hydrologic and biogeochemical monitoring. The south-facing 42-ha catchment is underlain by Rangeley mica schist, and outcrops are most prevalent along catchment boundaries. Bedrock is overlain by 0 to >6 m of glacial till and glacial drift derived primarily from Kinsman granodiorite (Bailey et al., 2003). The thickness of the parent materials is highly variable across short distances. Soils are generally sandy loams formed in till, and the average thickness of the solum is 0.6 to 0.8 m. Slopes are steep (average 30%), and there are no differences in slope among the five HPUs (Bailey et al., 2014). The climate is humid continental, with precipitation distributed evenly throughout the year. In summer and dry periods, there is little flow out of the catchment, but following precipitation events or snowmelt, high infiltration and hydraulic conductivity of the soil produce high-flow conditions in the groundwater and streams. Watershed 3 was last harvested for timber >100 yr ago, and the forest now consists of a mixture of American beech (*Fagus grandifolia* Ehrh.), sugar maple (*Acer saccharum* Marshall) and yellow birch (*Betula alleghaniensis* Britton) in deeper soils, and balsam fir [*Abies balsamea* (L.) Mill.] and red spruce (*Picea rubens* Sarg.) in shallow soils. The understory is dominated by hobblebush (*Viburnum lantanoides* Michx.), with a ground flora consisting of a variety of taxa including ferns, lycopods, and several members of the lily family.

Soil Description and Sampling

Throughout Watershed 3 (WS3), 99 soil profiles were observed and sampled following excavation of a small pit (<1 by 1 m) by hand (Fig. 1). The soil morphology was described according to standard field procedures (Schoeneberger et al., 2012). A total of 227 spodic B horizons from the 99 pedons were described and sampled. The soil profiles were collected by a variety of researchers. In the summers of 2008 and 2009, 59 pedons were collected by Bailey et al. (2014). For the earliest samples, representative horizon samples were collected except that only the upper 10 cm of the B horizon was sampled. For the remaining samples collected by Bailey et al. (2014) and subsequent researchers, representative samples for all described horizons were collected. In summer 2009, 17 additional pedons were observed and sampled by K. Harvey and S. Bailey (unpublished data) along three transects, each straddling a stream channel. Then, in summer 2011, 13 more pedons were observed in WS3. Finally, in summer 2012, 10 pedons were described and sampled intensively (approximately every 5 cm of depth within each horizon) (Fig. 1 and 2). These pedons were observed along three different catenas and together included at least one of each of the five HPUs (Fig. 2). Locations for the catenas were chosen based on prior knowledge of the soils and water table regime. Each catena was constructed with three to four pedons intended to capture two endmember HPUs and a transition zone between them. A clod of soil (with its original orientation preserved) was collected from spodic horizons from each of the 10 pedons and wrapped in aluminum foil for preparation of thin sections.

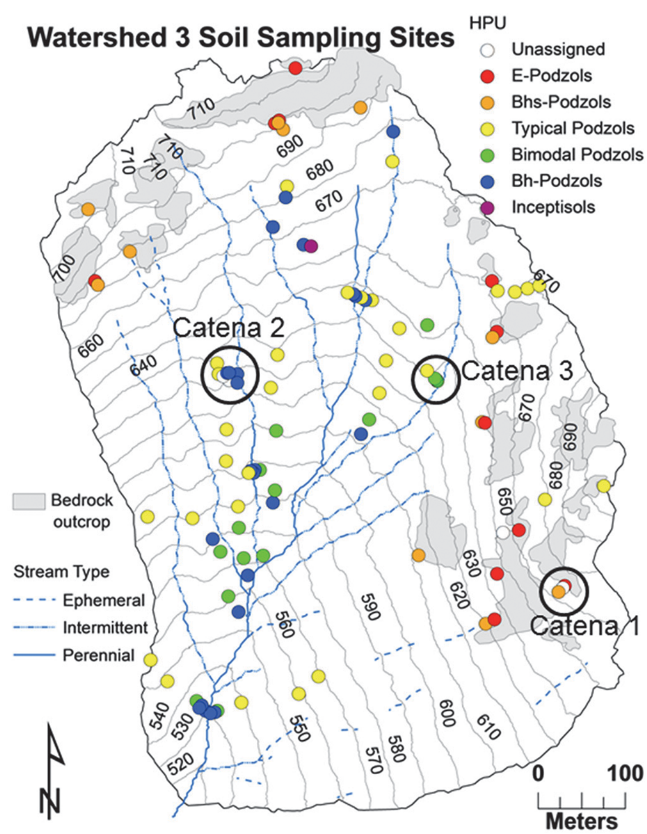

Fig. 1. Map of Watershed 3 at Hubbard Brook Experimental Forest, showing soil sampling locations, hydropedologic unit (HPU) designations, bedrock outcrops, and streams/stream types. Also shown are locations of Catenas 1, 2, and 3. Contours show elevation in meters. *Unassigned* refers to transitional soil profiles that did not fit the central concept of any HPU.

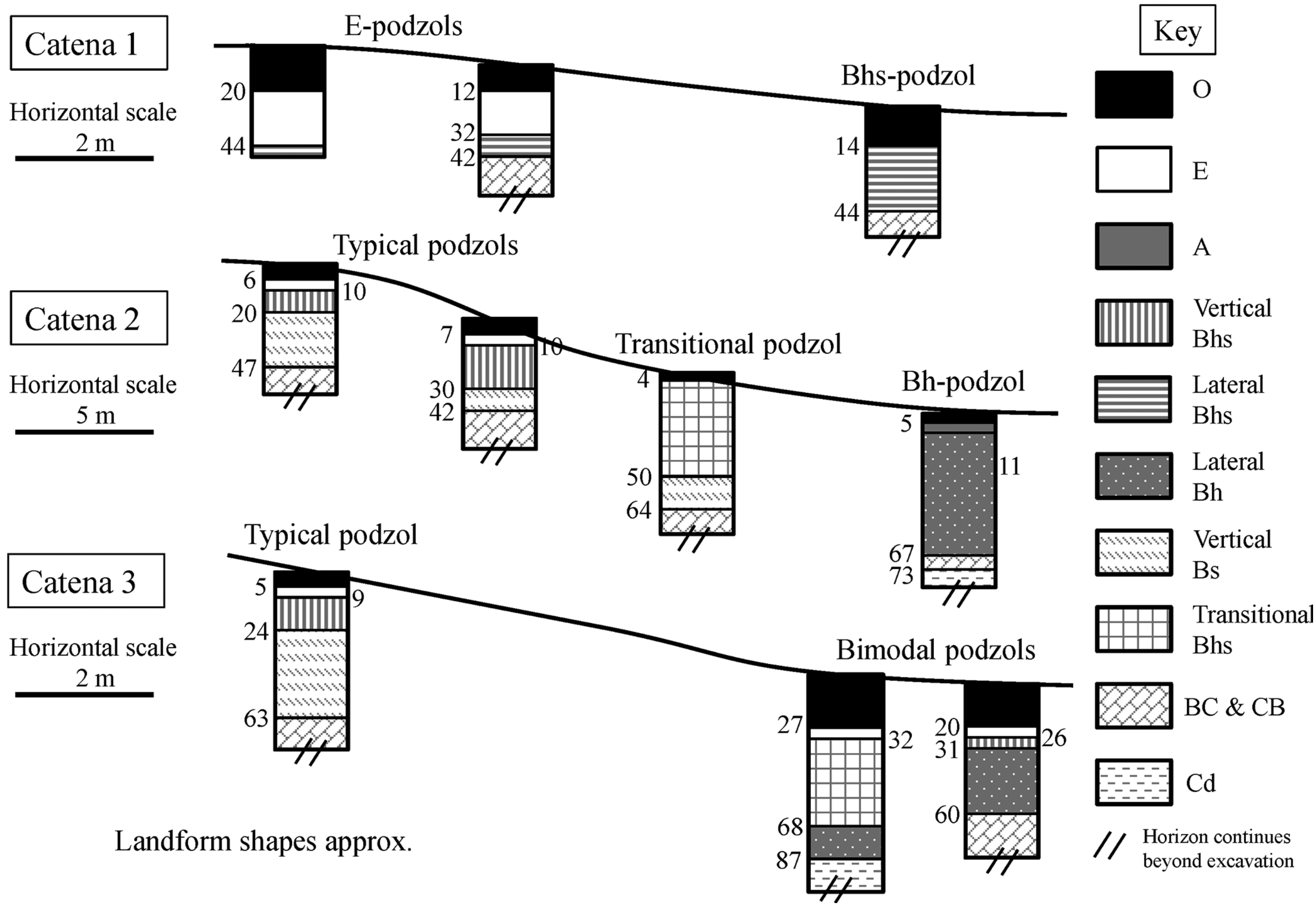

Fig. 2. Vertical cross-sections of Catenas 1, 2, and 3. Simplified horizonation is shown, with horizon boundaries shown in centimeters. Relative elevations are not to scale, and landform shapes are approximate.

Chemical Analyses

All soil samples were air dried and sieved to 2 mm to remove coarse fragments and ensure homogeneity. Small subsamples were ground with an agate mortar and pestle to pass through a 250-µm sieve and then extracted with citrate–dithionite (d) and acid ammonium oxalate (o) (Courchesne and Turmel, 2007). For the 10 intensively sampled soil profiles, subsamples were analyzed separately but averaged by horizon for horizon-based comparisons. All O horizons, and one-fourth of the mineral horizons were duplicated to ensure low experimental error (<10% for oxalate extracts and <5% for dithionite extracts). Extracts were diluted to one-fifth concentration and analyzed for Al_o, Fe_o, Fe_d, and Mn_d using a PerkinElmer inductively coupled plasma–atomic emission spectrometer. The optical density of oxalate extract (ODOE) was measured using a spectrophotometer at 430 nm as an assessment of C associated with spodic materials (Soil Survey Staff, 2004). Extraction of Al and Fe from soil with acid ammonium oxalate theoretically dissolves any Al–organic or Fe–organic complexes and releases soluble OM, which colors the extract a yellowish brown and can be quantified with absorbance of the extract. Extracts with absorbance exceeding the instrument's range were diluted to one-fifth concentration. Total organic C content was determined by dry combustion on a C.E. Elantech NC Soils Analyzer. Soil pH was measured for each horizon with a glass electrode in 2:1 (v/w) 0.01 mol L^{-1} $CaCl_2$/air-dry soil (Thomas, 1986). Most of the data (except pH) were positively skewed, so these were logarithmically transformed before analysis to approximate a normal distribution. Analyses of variance for chemical variables were performed in JMP Pro 9 (SAS Institute).

Thin Section Preparation and Analysis

Soil clods collected for thin section preparation were unwrapped and placed in a plastic cup with their original orientation preserved. The clods were air dried at room temperature and then dried overnight in a drying oven at 105°C. Clods were impregnated with Scotchcast no. 3 electrical resin (3M) in a vacuum desiccator to remove trapped air, and the resin was cured overnight in a drying oven at 105°C. Eighteen cured clods were shipped to Spectrum Petrographics, Vancouver, WA, for preparation into 30-µm thin sections, evenly polished for microprobe analysis.

The thin sections were observed and digitally photographed on a petrographic microscope. The thin sections were then sputter-coated with C and analyzed on a JEOL 6060 scanning electron microscope at 20 kV with a working distance of 10 mm. For each slide, 10 backscattered electron images (sites of interest) were captured at 500×. The location of each site of interest was selected haphazardly and chosen such that AOC would mostly fill the field of view. Amorphous organometallic complexes appeared as dark gray, fine material in the backscattered electron image, distinct from silt- and sand-sized mineral particles that had lighter, more uniform shades of gray and well-defined edges. A pixel-based map was created for each site of interest using scanning electron microscope–energy dispersive X-ray spectroscopy (SEM-EDS), which was then used to quantify the total elemental composition for each pixel using INCA Suite Version 4.15 (Oxford Instruments Analytical Ltd.). Each site of interest contained a variety of materials, including weathered and unweathered mineral grains, AOC, organic matter, and void space filled with resin. Therefore, point-based measurements were analyzed to quantify the elemental composition of the AOC only. Ten point measurements of total AOC elemental composition were analyzed per site of interest, for a total of 100 point measurements of AOC per slide; these were averaged to produce a mean value per slide. For quantification, a fixed list of 14 common elements (including C) was selected, and the total was normalized to 100%. However, the elemental compositions were considered imprecise because the C coating on the slides artificially elevated the intensity of the C spectrum. It was decided to include C in the quantification because there is much C in AOC, and removing it would strongly and artificially increase the normalized concentrations of other common elements such as Al and Fe. To remove some influence of the C coating, 18 haphazardly selected quartz grains were quantified because pure quartz theoretically contains only Si and O. The average C concentration of the quartz was 10.42% (with a standard deviation of 2.12%), and this was subtracted from the C concentration determined in the AOC. The other elements were then multiplied by 1.1042 to normalize the quantification to 100% after adjusting for the C coating. Non-normalized concentrations were not reported because the sum total of 14 elements often differed markedly from 100%, and the total non-normalized percentage varied widely among slides. Another potential source of error in the SEM-EDS quantification lies with the standardization procedure. Minerals were used to standardize the SEM-EDS, and quantification of elements in the less-dense AOC may have been affected. However, standards for this type of material do not exist.

To determine quantitative differences between the micromorphologies of different types of spodic horizons, color threshold analysis in ImageJ Version 1.47 (National Institutes of Health) was performed on 180 images (10 images for each of 18 horizon thin sections). Total porosity was determined as the void space percentage, identified as black areas in the backscattered electron image. Areas of the image covered by AOC and mineral grains were calculated using measurements of the percentage of the area covered by light gray mineral grains and darker gray AOC. Mean values for each slide are reported.

RESULTS

Morphology and Micromorphology of Spodic Horizons

It was expected that spodic horizons with different subhorizon designations and HPU membership in WS3 would differ with respect to their morphological properties. Indeed, the horizons were first differentiated in the field based on morphological characteristics such as matrix color. However, a simplified classification of spodic horizon types (related to but separate from HPU designation) and quantitative methods were needed to substantiate the field designations and to determine if the various spodic horizons were formed by different processes.

Four spodic horizon types were separated based on soil color and HPU membership (Table 1). The first spodic horizon type was the vertically developed Bhs horizon (VBhs) and was the most common type found in WS3. Vertically developed Bhs horizons had a Munsell hue of 7.5YR or redder and value and chroma both <3 (Table 1). These horizons were found in typical podzols or the upper part of bimodal podzols and were presumed to be developed via traditionally described pedon-scale podzolization by downward-percolating water. The other vertically developed spodic horizon type identified was the Bs horizon (VBs), which had a hue of 7.5YR or redder and a value or chroma >3 (Table 1). These VBs horizons were thicker than VBhs horizons (Table 2) and were always found below Bhs horizons in typical podzols and sometimes found below Bhs horizons in bimodal podzols. The next spodic horizon type identified was the laterally developed Bhs horizon (LBhs), which had a color similar to the vertically developed Bhs horizon (Tables 1 and 2) but was found in Bhs-podzols, a position predicted to receive AOC translocated laterally from E-podzols upslope. Individual LBhs horizons, as well as the combined thickness of all LBhs horizons per Bhs-podzol profile, tended to be twice as thick as individual VBhs horizons or combination of VBhs horizons in a typical or bimodal podzol profile (Table 2). The last spodic horizon type identified was the laterally developed Bh horizon (LBh), which had a hue of 10YR and a value and chroma both <3 (Table 1). This horizon type was found in Bh-podzols and the lower part of bimodal podzols in near-stream zones and benches predicted

Table 1. Hydropedologic unit (HPU) membership and field-moist Munsell color were used to group spodic horizons into four categories that denote the dominant direction of podzolization and the relative accumulation of illuvial humus and sesquioxides.

Spodic horizon type	HPUs containing type	Hue	Value	Chroma
Vertical Bhs	typical and bimodal podzols	7.5YR or redder	≤ 3	≤ 3
Vertical Bs	typical and bimodal podzols	7.5YR or redder	> 3 or ≥ 3 if chroma > 3	> 3 or ≥3 if value > 3
Lateral Bhs	E-podzols and Bhs-podzols	7.5YR or redder	≤ 3	≤ 3
Lateral Bh	Bh-podzols and bimodal podzols	10YR	≤ 3	≤ 3

Table 2. Munsell color, thickness, and total thickness of horizon type per soil profile of four different types of spodic horizons in WS3.

Spodic horizon type	n†	Munsell hue	Munsell value	Munsell chroma	Thickness of individual horizons	Thickness of all horizons of type per soil profile
					——— cm ———	
Vertical Bhs	76 (51)	7.5YR (49)‡ 5YR (24) 2.5YR (2) N (1)	2.7 ± 0.1 bc§	1.9 ± 0.1 b	11 ± 1 b	16 ± 2 b
Vertical Bs	36 (26)	7.5YR (23) 10YR (11)	3.4 ± 0.1 a	4.0 ± 0.1 a	18 ± 2 a	25 ± 3 b
Lateral Bhs	38 (21)	7.5YR (27) 5YR (9) 10YR (2)	2.8 ± 0.1 b	2.1 ± 0.1 b	21 ± 2 a	39 ± 3 a
Lateral Bh	77 (40)	10YR (65) 7.5YR (7) 5YR (2) 2.5Y (1)	2.5 ± 0.1 c	2.1 ± 0.1 b	20 ± 1 a	37 ± 2 a

† Number of individual genetic horizons observed, with the number of soil profiles containing the given spodic horizon type in parentheses.
‡ Number of horizons displaying the hue within each spodic horizon type in parentheses.
§ Means ± standard errors are reported for Munsell value and chroma and horizon thicknesses; those in the same column followed by the same letter are not significantly different ($\alpha = 0.05$).

to accumulate laterally deposited AOC. These LBh horizons, and the combined thickness of all LBh horizons in a Bh-podzol, had thickness similar to LBhs horizons (Table 2). Therefore, laterally developed spodic horizons as a whole tended to be twice as thick as vertically developed Bhs horizons. Buurman et al. (2013) also found thicker spodic horizons in the most poorly drained members of an Amazonian catena with predominantly lateral flow. A few pedons observed in WS3 appeared to be transitional between having predominantly vertical or lateral flow and did not seem to fit the central concept of any HPU. In these cases, the pedon was classed as unassigned or the HPU most similar (Fig. 1), and one or more spodic horizons were considered transitional types (Fig. 2).

Morphological differences among spodic horizon types were also observed qualitatively and quantitatively at the microscale in thin section. For example, VBhs horizons tended to show darker, redder colors and a well-developed microstructure, with spodic (AOC) pellets forming distinct microaggregates, also called *crumb microstructure* (Fig. 3 and 4), which is considered typical of spodic horizons (McKeague et al., 1983; McSweeney and FitzPatrick, 1990; Condron and Rabenhorst, 1992; Bardy et al., 2008). Another way of describing the microstructure is the coarse/fine (c/f)-related distribution, which is a qualitative description of the relationship between coarse (sand and silt grains) and fine materials (AOC in this case) (Stoops, 2003). Vertically developed Bhs horizons had a c/f-related distribution that was double-spaced, fine to coarse enaulic, which also describes a crumb microstructure and is common for spodic horizons (Stoops, 2003). These qualitative observations were confirmed by a higher AOC/mineral ratio and greater total porosity in VBhs horizons relative to all other spodic horizon types (Table 3). The LBh horizons tended to show a yellower hue and fine materials that formed a more infilled microstructure with a massive appearance (Fig. 3 and 4). These laterally developed spodic horizons tended to have a c/f-related distribution best described as single- to double-spaced porphyric. Compared with VBhs horizons, LBh horizons had a similar AOC/mineral ratio but less total porosity (Table 3).

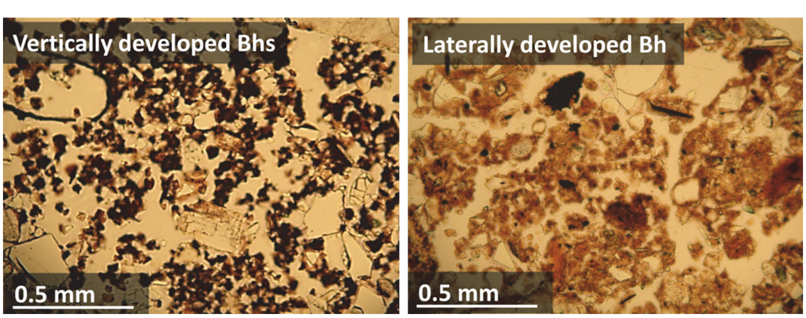

Fig. 3. Microphotographs of a vertically developed Bhs horizon (left) and a laterally developed Bh horizon (right) from the same hillslope under plane-polarized light. Note the contrasting color and different structure of amorphous organometallic complexes (fine material). Vertically developed Bhs horizons had a well-developed crumb microstructure dominated by spodic microaggregates (double-spaced fine to coarse enaulic coarse/fine-related distribution). Laterally developed Bh horizons had a more infilled structure (single- to double-spaced porphyric coarse/fine-related distribution).

Vertically developed Bhs and laterally developed Bhs horizons, although morphologically similar at the pedon scale, showed distinct differences at the microscale. Laterally developed Bhs horizons tended to have colors similar to VBhs horizons, but their microstructure was more similar to LBh horizons. Laterally developed Bhs horizons had significantly lower AOC/mineral ratios and less total porosity than VBhs horizons (Table 3).

Chemical Composition of Spodic Horizons

Vertically developed Bhs and LBhs horizons had the highest concentrations of organic C and Fe (Table 4), while VBs and LBh horizons had the greatest concentrations of Al (Tables 4 and 5). The optical density of oxalate extract (ODOE) was significantly higher in VBhs horizons than all other spodic horizon types (Table 4). The VBs horizons, although also vertically developed, had low ODOE values due to low organic C concentrations (Table 4). Even though LBhs and LBh horizons had darker colors that would suggest high concentrations of illuvial C (Tables 1 and 2), these horizons actually had relatively lower ODOE and concentrations of organic C than VBhs horizons (Table 4).

In general, the chemical extractions and SEM-EDS methods agreed with regard to relative trends for C, Fe, and Al in the four spodic horizon types (Tables 4 and 5). However, there were no statistically significant differences between spodic horizon types for C or Fe determined by SEM-EDS. The concentrations of Al, Fe, and Mn tended to be greater in the bulk soil (Table 4) (using dithionite and oxalate extractions) than in the AOC themselves (Table 5) (using SEM-EDS). Aluminum in AOC measured by SEM-EDS was correlated with Al_o in the bulk soil samples ($r = 0.48$, $P = 0.04$). Iron in AOC measured by SEM-EDS and Fe_o in the bulk soil had no significant correlation ($r = 0.28$, $P = 0.26$). Manganese in AOC measured by SEM-EDS and Mn_d in the bulk soil were correlated ($r = 0.63$, $P = 0.005$).

Classification of Vertically vs. Laterally Developed Podzols

Many of the pedons observed did not have an albic horizon, so chemical criteria had to be used in addition to color requirements for spodic materials. Only the uppermost spodic horizon was considered for these classification criteria, as required by the USDA soil taxonomy. Because VBs horizons always occurred below VBhs horizons, they were not used for classification (Table 6). Pedons for which a VBhs horizon was used for classification had the highest proportional differences in ODOE and Al + 0.5Fe between the surface horizon and the spodic horizon (Table 6). Therefore, pedons containing a VBhs horizon were classified as Spodosols 96% of the time (Table 6). Pedons containing an LBhs or LBh as the uppermost spodic horizon had relatively lower proportional differences in ODOE and Al + 0.5Fe between the surface horizon and the spodic horizon, and only 50% of these pedons met the criteria for Spodosols (Table 6).

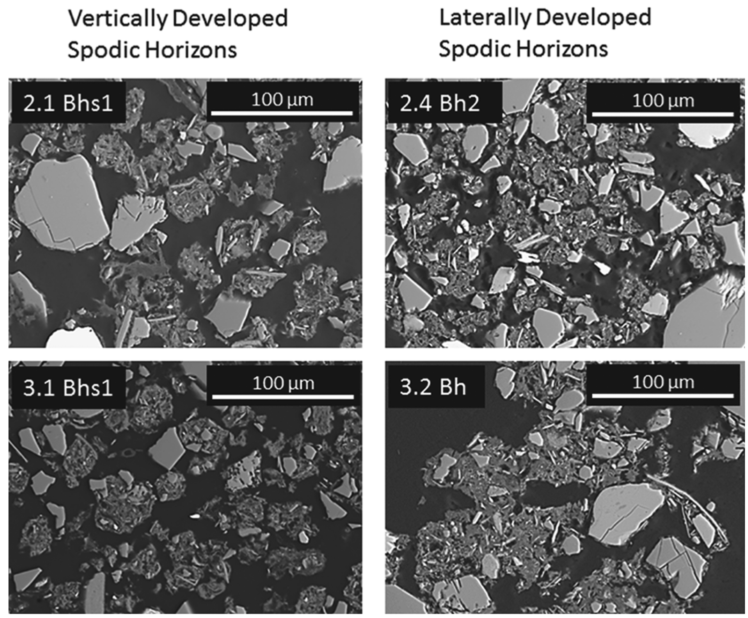

Fig. 4. Backscattered electron images produced using a scanning electron microscope. Vertically developed Bhs horizons had a higher ratio of amorphous organometallic complexes to mineral grains (by area) and greater total porosity than laterally developed spodic horizons.

DISCUSSION

Morphology and Micromorphology of Spodic Horizons

Soil morphology is the net expression of past and current soil-forming factors and the resulting soil-forming processes. The differences in morphology, specifically the color, thickness (Table 2), and microstructure (Fig. 3 and 4), among the various types of spodic horizons (VBhs, VBs, LBhs, and LBh) suggest that there are differences in the soil-forming factors and/or processes leading to their formation. In WS3, HPUs were defined based on morphology, which was shown to vary due to differences in the water table regime caused by topographic characteristics (Bailey et al., 2014; Gannon, 2014). Therefore, we interpreted morphological and micromorphological differences between spodic horizon types as resulting from differences in pedogenic processes among HPUs.

When interpreting the porosity results (Table 3), it should be noted that depth in the soil profile is a potential confounding factor because the tendency is for bulk density to increase and porosity to decrease with depth. However, there was no significant difference among sampling depths for the four spodic

Table 3. Sampling depth, ratio of amorphous organometallic complexes (AOC) to mineral grains by area, and total porosity of four different types of spodic horizons. The AOC/mineral ratio and total porosity were determined by color threshold analysis of scanning electron microscope backscattered images in ImageJ software. Qualitative description of predominant coarse/fine (c/f)-related distribution according to terminology of Stoops (2003).

Horizon type	*n*	Depth	AOC/mineral ratio†	Total porosity	c/f-related distribution
		cm		%	
Vertical Bhs	7	23 ± 7 a†	1.32 ± 0.11 a	50 ± 4 a	double-spaced, fine to coarse enaulic
Vertical Bs	3	42 ± 10 a	0.89 ± 0.18 ab	48 ± 1 ab	single-spaced fine enaulic; single-spaced porphyric
Lateral Bhs	3	36 ± 9 a	0.70 ± 0.30 b	42 ± 4 b	single- to double-spaced porphyric; single-spaced chitonic
Lateral Bh	4	53 ± 9 a	1.10 ± 0.14 ab	42 ± 1 b	single- to double-spaced porphyric

† Means ± standard errors; those in the same column followed by the same letter are not significantly different ($\alpha = 0.05$).

Table 4. Chemical extraction data on organic C, citrate–dithionate-extractable Fe and Mn (Fe_d and Mn_d, respectively), oxalate-extractable Fe and Al (Fe_o and Al_o, respectively), optical density of oxalate extract (ODOE), and pH in 0.01 mol L^{-1} $CaCl_2$ for four different types of spodic horizons in Watershed 3.

Horizon type	*n*	Organic C	Fe_d	Fe_o	Al_o	Mn_d	ODOE	pH
		mg kg^{-1}					absorbance	
Vertical Bhs	66	55,814 ± 241 a†	15,863 ± 793 a	12,649 ± 690 a	7596 ± 532 b	66 ± 65 b	2.63 ± 0.13 a	3.86 ± 0.04 c
Vertical Bs	20	37,381 ± 420 b	11,932 ± 1401 ab	9749 ± 1195 ab	10,347 ± 922 a	88 ± 113 ab	1.48 ± 0.23 b	4.45 ± 0.07 a
Lateral Bhs	33	47,870 ± 335 ab	14,437 ± 1113 a	12,199 ± 953 ab	7537 ± 735 ab	424 ± 90 ab	1.81 ± 0.18 b	3.94 ± 0.07 c
Lateral Bh	63	44,927 ± 237 b	10,378 ± 790 b	8116 ± 674 b	8394 ± 520 ab	405 ± 64 a	1.47 ± 0.13 b	4.18 ± 0.05 b

† Means ± standard errors; those in the same column followed by the same letter are not significantly different (α = 0.05).

horizon types (Table 3). Therefore, the differences observed were probably the result of differences in hydropedology. The lower porosity and lower AOC/mineral ratio of LBhs and LBh horizons (Table 3) imply that they have higher bulk density than VBhs horizons, assuming similar particle density. Consequently, given equal gravimetric water contents, LBhs and LBh horizons should have lower water-holding capacity, greater volumetric water content, and less aeration than VBhs horizons.

Chemical Composition of Spodic Horizons

Differences in morphology among the four types of spodic horizons were reflected in general trends and statistical differences in the concentrations of the pedogenically significant elements C, Fe, Al, and Mn (Tables 4 and 5). However, there was little direct agreement between the wet chemical extraction of bulk soil samples (Table 4) and the total elemental composition of AOC in thin section by SEM-EDS (Table 5). When considering the differences between results from chemical extractions (Table 4) and SEM-EDS (Table 5), it must be noted that the methods were conducted at different scales and each had different sources of error and operational definitions, so it was expected that they would differ to some extent. Another possible explanation for the disparity between the two methods could be that there exists some Al, Fe, and Mn outside of AOC. These elements could take the form of concentrated oxides, organic forms, structural components of clays, or adsorbed or exchangeable forms not examined in this study.

Laterally developed Bh horizons were found in bimodal podzols and Bh-podzols in benches and near-stream zones (Table 1; Bailey et al., 2014), and this type of spodic horizon had some distinctive characteristics. The LBh horizons had very dark colors (Tables 1 and 2), hence the "h" designation, so it was originally suspected that they would have similar (or higher) C content and ODOE compared with Bhs horizons. However, LBh horizons had comparatively low concentrations of organic C and ODOE, similar to Bs horizons (Table 4). The LBh horizons lacked the reddish hue indicative of Fe oxides (Tables 1 and 2), and they had low concentrations of Fe relative to spodic horizons that had the "s" designation (Table 4). In vertically developed, typical podzols, VBs horizons had the highest concentrations of Al. This is because secondary Al is more mobile than Fe, and its maximum concentration tends to occur below the Fe maximum due to vertical translocation (Blume and Schwertmann, 1969). For Bh-podzols, however, the high concentration of Al (Tables 4 and 5) is probably due to lateral translocation and accumulation of this element with organic C in near-stream and bench zones, which has been documented in other podzolized landscapes (Sommer et al., 2001; Löfgren and Cory, 2010). The LBh horizons also had the greatest concentrations of Mn (Tables 4 and 5), which can be mobilized under humid, acid conditions such as those at Hubbard Brook. Therefore, we interpreted these results as translocation and accumulation of Mn in near-stream zones according to lateral flow paths.

Classification of Vertically vs. Laterally Developed Podzols

In the USDA soil taxonomy, a soil may be classified as a Spodosol only if specific criteria are met. In a frigid soil temperature regime with loamy soils (such as those found at Hubbard Brook), an uncultivated soil must have a spodic horizon with sufficient thickness (10 cm or more) or cementation in 50% or more of the pedon; a particle-size class of coarse-loamy, loamy-skeletal or finer; an upper boundary within 50 cm; and an overlying albic horizon in 50% or more of each pedon. A spodic horizon is an illuvial layer 2.5 cm or more thick comprised of at least 85% spodic materials. Spodic materials are mineral soil

Table 5. Normalized elemental contents of amorphous organometallic complexes from four different types of spodic horizons determined by scanning electron microscopy–energy dispersive X-ray spectroscopy.

Horizon type	*n*	C	Fe	Al	Mn
			mg kg^{-1}		
Vertical Bhs	7	$2.45 \times 10^4 \pm 1.51 \times 10^3$ a†	$9.20 \times 10^3 \pm 1.30 \times 10^3$ a	$6.72 \times 10^3 \pm 1.88 \times 10^3$ b	0‡ ± 24 ab
Vertical Bs	3	$1.97 \times 10^4 \pm 2.30 \times 10^3$ a	$6.53 \times 10^3 \pm 2.0 \times 10^3$ a	$1.04 \times 10^4 \pm 1.14 \times 10^3$ ab	8§ ± 37 ab
Lateral Bhs	3	$2.50 \times 10^4 \pm 2.00 \times 10^3$ a	$6.70 \times 10^3 \pm 1.71 \times 10^3$ a	$8.32 \times 10^3 \pm 9.91 \times 10^2$ ab	0‡ ± 32 b
Lateral Bh	4	$2.20 \times 10^4 \pm 2.00 \times 10^3$ a	$5.39 \times 10^3 \pm 1.71 \times 10^3$ a	$1.12 \times 10^4 \pm 991 \times 10^2$ a	71§ ± 32 a

† Means ± standard errors; those in the same column followed by the same letter are not significantly different (α = 0.05).

‡ Computed means were actually negative values, meaning that Mn was far below the detection limit of 100 mg kg^{-1}.

§ Below detection limit of 100 mg kg^{-1}.

materials dominated by illuvial, active, amorphous associations of Al and OM, with or without Fe (AOC). If an albic horizon is present, underlying spodic materials may be identified by color alone: a hue of 5YR or redder or a hue of 7.5YR, a value 5 or less, and a chroma 4 or less; a hue of 10YR or N and a value and chroma 2 or less; or a color of 10YR 3/1. However, if an albic horizon is not present, the soil material must have one of the colors listed above or a hue of 7.5YR, value of 5 or less, chroma or of 5 or 6, and one or more of the following properties: (i) cementation by OM and Al in 50% or more of the pedon and a very firm or firmer consistence; (ii) 10% or more cracked coatings on sand grains; (iii) oxalate-extractable $Al_o + 0.5Fe_o$ percentages of 0.50 or more and half that amount or less in an overlying umbric epipedon, ochric epipedon, or albic horizon; or (iv) an ODOE value of 0.25 or more and a value half as high or lower in an overlying umbric epipedon, ochric epipedon, or albic horizon (Soil Survey Staff, 2010). These definitions of spodic materials, spodic horizons, and Spodosols in the USDA soil taxonomy were developed assuming vertical, pedon-scale podzolization. The definitions emphasize the eluviation of Al and OM from the epipedon and albic horizon and vertical illuviation of AOC into the B horizon. This pedon-scale approach to classification may not be appropriate when eluvial and illuvial zones are separated on different portions of a hillslope. Consequently, classification of laterally developed podzols is problematic using the USDA soil taxonomy. Thus far, we have been using the general term *podzols* to describe soils in WS3 with spodic materials because some of them are not actually classified as Spodosols. The term *podzol* denotes that podzolization is an important soil-forming process but does not imply classification as a Spodosol. However, the term *podzol* is not generally used in the United States because it has no technical definition in the USDA soil taxonomy.

Table 6. Comparison of spodic horizon types used for the classification of the observed pedons. Proportional differences in optical density of oxalate extract (ODOE) and $Al_o + 0.5Fe_o$ are expressed as (spodic horizon value − surface horizon value)/spodic horizon value. Values >0.5 indicate that the value for the spodic horizon was twice as high as the overlying surface horizon (a value of 0.5 for either ODOE or $Al_o + 0.5Fe_o$ proportional difference defines Spodosol status in the absence of an albic horizon). The proportions of pedons meeting the classification criteria for Spodosols for each spodic horizon type are also shown.

Spodic horizon type used for classification of pedon	*n*	ODOE proportional difference	$Al_o + 0.5Fe_o$ proportional difference	Pedons meeting Spodosol criteria
				%
Vertical Bhs	49	0.7 ± 0.1 a†	0.8 ± 0.0 a	96
Lateral Bhs	18	0.2 ± 0.2 ab	0.5 ± 0.1 b	50
Lateral Bh	18	−0.1 ± 0.3 b	0.4 ± 0.1 b	50

† Means ± standard errors; those in the same column followed by the same letter are not significantly different ($\alpha = 0.05$).

In WS3, soils containing a VBhs horizon were almost always classified as Spodosols (Table 6). Vertically developed Bhs horizons occurred mostly in typical podzols, but they also sometimes occurred in the upper part of bimodal or Bh-podzols (Table 1). The VBhs horizon, because it was developed by vertical podzolization, fit the taxonomic definitions as intended. This allowed bimodal or Bh-podzols containing a VBhs horizon in the upper part to be classified as Spodosols. However, only about half of the podzols containing a laterally developed Bhs horizon or LBh horizon were classified as Spodosols (Table 6), despite the fact that Bhs-podzols and Bh-podzols appeared to have very well-developed spodic horizons due to their color and thickness (Table 2). Nonetheless, these laterally developed podzols diverged from vertically developed podzols in classification at the highest level of the USDA soil taxonomy half of the time (Table 6) because many of the Bhs-podzols and Bh-podzols (which had LBhs and LBh horizons, respectively) had no E horizon, relatively lower ODOE values in the spodic horizon (Table 4), and relatively little difference in ODOE and $Al_o + 0.5Fe_o$ between the spodic horizon and the surface horizon immediately overlying it (Table 6). Perhaps laterally deposited AOC had entered the surface horizons, which did not create the contrast between the epipedon (eluvial zone) and spodic horizons (illuvial zone) typical of vertical podzolization. Also, perhaps the lateral podzolization process produced more diffuse spodic materials with lower C content and ODOE than spodic materials produced by vertical podzolization. The fact that the Bh-podzols and Bhs-podzols did not often meet the criteria for Spodosol classification highlights one of the challenges with the USDA soil taxonomy, which assumes that soils form vertically at the pedon scale and does not take landscape-scale pedogenic processes into account. Fiedler et al. (2002) also came to the conclusion that soil function is not sufficiently captured by current soil classification systems and that a review of such systems is warranted for soils developed at the hillslope scale.

Vertical vs. Lateral Modes of Podzolization

We propose that there are at least two distinct modes of podzolization occurring in WS3. The first, most common, and familiar mode is vertical podzolization, which is thought to occur in all typical podzols and in the upper part of bimodal podzols. These two HPUs show common New England Spodosol morphology, with discontinuous E horizons and relatively thin, wavy Bhs horizons underlain by Bs horizons. Although the exact mechanisms of podzolization have yet to be fully elucidated, its general process is well documented and accepted. The classical theory of podzolization was developed assuming vertical, unsaturated flow and vertical horizon development. Typical podzols almost always experience vertical, unsaturated flow, and bimodal podzols experience this condition in the upper part (Bailey et al., 2014). The well-developed crumb (enaulic) structure of spodic pellets (Fig. 3 and 4) and higher total porosity of VBhs horizons (Table 3) suggest freely percolating water and precipitation of AOC around nucleation centers via classical podzolization.

The second mode is lateral podzolization. Because of their distinct morphology (Table 2), micromorphology (Table 3; Fig. 3 and 4), chemical composition (Tables 4 and 5), and water table dynamics (Bailey et al., 2014), Bhs-podzols, Bh-podzols, and the lower Bh horizons of bimodal podzols are thought to develop via lateral podzolization in WS3. Although others have documented the occurrence of lateral podzolization (Sommer et al., 2000, 2001; Bardy et al., 2008; Lucas et al., 2012; Buurman et al., 2013; Bailey et al., 2014; Jankowski, 2014), there has not yet been a thorough explanation of the pedogenic process and comparison with vertical podzolization processes. In WS3, the most obvious example of lateral podzolization is found in the E- and Bhs-podzols, represented by Catena 1 (Fig. 2). These soils occur in very close proximity to each other, and the transition zone between them can be quite narrow (1–2 m). Buurman et al. (2013) found abrupt transitions between well-drained and poorly drained podzols in the Amazon and suggested a positive feedback between soil formation and impeded drainage due to lateral accumulation of dissolved OM and precipitation of AOC in pores. Similarly, in the case of development of E-podzols and Bhs-podzols at Hubbard Brook, we suggest that lateral podzolization probably occurs via solutional transport of Al^{3+} and dissolved organic C (DOC) downslope with groundwater, followed by complexation of Al^{3+} and DOC and precipitation and immobilization. This idea is supported by WS3 well and lysimeter data, which show a decrease in groundwater and soil water DOC from E- to Bhs-podzols (Zimmer et al., 2013), probably as laterally transported DOC becomes adsorbed by or precipitated as AOC. Sommer and Schlichting (1997) presented a classification of catenas based on landscape-scale pedogenic processes (translocations, transformations, additions, and losses). Bailey et al. (2014) suggested that the hillslope development of E- to Bhs-podzols represents a solutional downward translocation catena according to the terminology of Sommer and Schlichting (1997).

The typical podzol–bimodal podzol–Bh-podzol hillslope sequence, represented by Catenas 2 and 3 (Fig. 2) also shows evidence of lateral podzolization. In these catenas, the eluvial zone (O and E horizons) decreases in thickness downslope, while the illuvial zone (B and BC horizons) increases in thickness. Sommer et al. (2001) quantified this as an increasing illuviation–eluviation ratio, indicating lateral podzolization, and WS3 shows similar patterns. Solutional transport of Al^{3+}, other metals, and DOC could also produce the morphology observed in the typical podzol to Bh-podzol catena. Extended lateral transport of Al^{3+}, Fe^{3+}, Mn^{2+}, and DOC could be facilitated under acid conditions and saturation of soil exchange sites. Fiedler et al. (2002) suggested that redox gradients in their study site accounted for lateral transport and downslope accumulation of Mn, Fe, and organic C. At our site, however, there are very small differences in pH between spodic horizon types (Table 4), and there was no downslope pH gradient in the three catenas. In addition, increasing water table heights with decreasing elevation suggest that, if there is a redox gradient, the soils would become more reducing toward the stream, and thus there would be less accumulation of metals and organic C downslope. Therefore, it seems unlikely that a redox gradient is causing lateral transport in WS3.

Another possible mechanism of lateral podzolization in the typical podzol–bimodal podzol–Bh-podzol hillslope sequence (Fig. 2) is a physical translocation or lateral illuviation of previously precipitated AOC from upslope to downslope. Observations of HPUs along catenas (Fig. 2) show that the Bh horizon increases in thickness from upslope to downslope in near-stream and bench areas, and the presence of Bh materials at the B–C interface in bimodal podzols and Bh-podzols could suggest a physical deposition from upslope. Analysis of micromorphology may also support the hypothesis of physical transport. The massive (porphyric) microstructure of AOC and lower porosity of Bh horizons (Fig. 3 and 4) could indicate that physically transported AOC have filled in the voids between mineral grains. Bardy et al. (2008) documented similar microstructure in waterlogged, laterally developed spodic horizons in the Amazon basin. Unsaturated and/or saturated lateral flow in the solum could physically transport colloidal AOC through pore spaces. In WS3, Gannon (2014) provided evidence for lateral unsaturated flow above the water table in horizons presumed to be developed via lateral podzolization. Jankowski (2014) suggested that hydrophobicity of the spodic horizon itself may enhance lateral gradients in unsaturated flow. Amorphous organometallic complexes could be physically flushed sporadically during precipitation events or snowmelt, when lateral flux is most likely. Amorphous organometallic complexes would then accumulate via interception by soil particles, which would filter them from the soil water or groundwater en route to the stream. Because the lower portion of the Bh horizon is often saturated (40–60% of the time) but the upper portion of the Bh horizon is rarely saturated (Bailey et al., 2014), both unsaturated and saturated flow could be transporting and depositing colloidal AOC in the lower part of the solum. This process would create a bimodal podzol or Bh podzol depending on the thickness of lateral accumulation of AOC. The typical podzol–bimodal podzol–Bh-podzol hillslope sequence (Fig. 2) could therefore represent a solid-phase downward translocation catena, according to the terminology of Sommer and Schlichting (1997). To determine whether lateral podzolization occurs as solutional or solid-phase transport, a future study would have to analyze pore water and groundwater composition (particulates + solutes). It is also possible that both solutional and solid-phase transport happen simultaneously or alternately with fluctuations in water table and activation of vertical vs. lateral gradients. However, it would be difficult to determine the ultimate source of any particulates or solutes in the water. In this case, a future study could develop a controlled laboratory or field tracer experiment to test the hypotheses.

Soils are known to be dynamic natural bodies that change in space and time, but it is very difficult to date pedogenic processes. It is not known how soil morphology in WS3 has changed with time since the beginning of pedogenesis with the retreat of the glaciers approximately 14,000 yr ago. Recently, some have suggested that depodzolization may be occurring in eastern forests due to timber harvest and climate change, resulting in the loss of spodic materials and changes in soil morphology over a short period of time (Barrett and Schaetzl, 1998; Teets and Nowacki, 2012). Watershed 3 was harvested approximately 100 yr ago and, at Hubbard Brook, it has been shown that acid deposition has accelerated exports of Al^{3+} (Driscoll and Postek, 1996). Perhaps lateral podzolization is actually a recent phenomenon resulting from depodzolization following past deforestation and acid deposition. It has been suggested that acid rain has altered podzolization by facilitating the transport of inorganic Al to surface waters through complexation with inorganic anions such as SO_4^{2-}, especially during snowmelt (Driscoll et al., 1985, 2001). The loss of Al^{3+} and other chelating metals could result in decomplexation of AOC and the transport of Al and OM down the soil profile (perhaps creating a bimodal podzol) or downslope toward the stream, followed by reprecipitation of AOC with increased pH or sorption onto existing AOC. Near-stream soils (Bh-podzols) with Bh horizons could thus be generated or enhanced by depodzolization through acting as a pedochemical barrier (Sommer et al., 2001) for some or all components of AOC. This hypothesis could perhaps be tested in a future long-term study examining podzolization–depodzolization trends in terms of soil morphology and soil water chemistry.

CONCLUSIONS

The soils of Watershed 3 at Hubbard Brook Experimental Forest, New Hampshire, showed two distinct modes of podzolization: vertical and lateral. The dominant mode of podzolization occurring in a given pedon depended on the dominant groundwater flux direction. Vertically developed and laterally developed spodic horizons differed with respect to their morphological and chemical properties. In addition, they appeared to have different pedogenic processes, which led to differences in classification. Laterally developed spodic horizons were usually twice as thick as vertically developed spodic horizons and contained higher concentrations of Al and Mn but lower concentrations of Fe and C. Vertically developed spodic horizons had a well-developed crumb (enaulic) microstructure, while laterally developed spodic horizons often had a more infilled, massive (porphyric) microstructure. In addition, vertically developed spodic horizons had higher porosity and AOC/mineral ratios than laterally developed spodic horizons. Laterally developed podzols often lacked an obvious eluvial zone, which was actually found in the soils upslope. As a result, concentrations of Al, Fe, and spodic C in the eluvial horizons of laterally developed podzols were often relatively high and lacked sufficient contrast with the spodic horizon, making classification as Spodosols problematic. Lateral pedogenesis has not received as much attention from pedologists as vertical pedogenesis. However, this study demonstrates that lateral horizon formation should not be ignored, especially in catchments or hillslopes predicted or documented to have lateral flux of water and solutes. Spatial variations in soil morphology and soil chemistry may be attributed to lateral as well as vertical pedogenesis in such podzolized catchments at Hubbard Brook. Future hydropedologic or biogeochemical studies should take this into account to model processes and spatial variations more accurately.

ACKNOWLEDGMENTS

We wish to thank colleagues Kevin McGuire, J.P. Gannon (Virginia Tech) and Tom Bullen (USGS) for collaborative ideas; Michele Von Turkovich (UVM) for technical assistance with SEM-EDS; and undergraduate assistants Noah Ahles, Andrea Brendalen, Silene DeCiucies, Ethan Morehouse, Emily Piché, and Geoff Schwaner for field and laboratory assistance. Many thanks to two anonymous reviewers for comments on an earlier version of this manuscript. This work was supported by NSF EAR Hydrologic Sciences 101450, and was completed as part of the dissertation requirement for R.R. Bourgault. Hubbard Brook Experimental Forest is operated and maintained by the U.S. Forest Service, Northern Research Station, Newtown Square, PA.

REFERENCES

Bailey, S.W., P.A. Brousseau, K.J. McGuire, and D.S. Ross. 2014. Influence of hillslope position and transient water table on soil development and carbon distribution in a steep, headwater catchment. Geoderma 226–227:279–289. doi:10.1016/j.geoderma.2014.02.017

Bailey, S.W., D.C. Buso, and G.E. Likens. 2003. Implications of sodium mass balance for interpreting the calcium cycle of a forested ecosystem. Ecology 84:471–484. doi:10.1890/0012-9658(2003)084[0471:IOSMBF]2.0.CO;2

Bardy, M., E. Fritsch, S. Derenne, T. Allard, N.R. do Nascimento, and G.T. Bueno. 2008. Micromorphology and spectroscopic characteristics of organic matter in waterlogged podzols of the upper Amazon basin. Geoderma 145:222–230. doi:10.1016/j.geoderma.2008.03.008

Barrett, L.R., and R.J. Schaetzl. 1998. Regressive pedogenesis following a century of deforestation: Evidence for depodzolization. Soil Sci. 163:482–497. doi:10.1097/00010694-199806000-00006

Bishop, K.H., U.S. Lundström, and R. Giesler. 1993. Transfer of organic C from forest soils to surface waters: Example from northern Sweden. Appl. Geochem. 8(Suppl. 2):11–15. doi:10.1016/S0883-2927(09)80003-6

Blume, H.P., and U. Schwertmann. 1969. Genetic evaluation of profile distribution of aluminum, iron, and manganese oxides. Soil Sci. Soc. Am. Proc. 33:438–444. doi:10.2136/sssaj1969.03615995003300030030x

Buurman, P., P. Vidal-Torrado, and V.M. Martins. 2013. The podzol hydrosequence of Itaguaré (São Paulo, Brazil): 1. Geomorphology and interpretation of profile morphology. Soil Sci. Soc. Am. J. 77:1294–1306. doi:10.2136/sssaj2012.0080

Condron, M.A. and M.C. Rabenhorst. 1992. Micromorphology of spodic horizons in a Psamment–Aquod toposequence on the Atlantic Coastal Plain of Maryland, U.S.A. Dev. Soil Sci. 22:179–186.

Courchesne, F., and M.-C. Turmel. 2007. Extractable Al, Fe, Mn, and Si. p. 307–315. In: M.R. Carter and E.G. Gregorich, editors, Soil sampling and methods of analysis. 2nd ed. CRC Press, Boca Raton, FL.

Dahlgren, R.A., and F.C. Ugolini. 1989. Formation and stability of imogolite in a tephritic Spodosol, Cascade Range, Washington, USA. Geochim. Cosmochim. Acta 53:1897–1904. doi:10.1016/0016-7037(89)90311-6

Drever, J.I., and L.L. Stillings. 1997. The role of organic acids in mineral weathering. Colloids Surf. A 120:167–181. doi:10.1016/S0927-7757(96)03720-X

Driscoll, C.T., G.B. Lawrence, A.J. Bulger, T.J. Butler, C.S. Cronan, C. Eagar, et al. 2001. Acidic deposition in the northeastern United States: Sources and inputs, ecosystem effects, and management strategies. BioScience 51:180–198. doi:10.1641/0006-3568(2001)051[0180:ADITNU]2.0.CO;2

Driscoll, C.T., and K.M. Postek. 1996. The chemistry of aluminum in surface waters. In: G. Sposito, editor, The environmental chemistry of aluminum. CRC Press, Boca Raton, FL. p. 363–418.

Driscoll, C.T., N. van Breemen, and J. Mulder. 1985. Aluminum chemistry in a forested Spodosol. Soil Sci. Soc. Am. J. 49:437–444. doi:10.2136/sssaj1985.03615995004900020033x

Fanning, D.S., and M.C.B. Fanning. 1989. Soil morphology, genesis, and classification. John Wiley & Sons, New York.

Fiedler, S., H.P.F. Jungkunst, R. Jahn, M. Kleber, M. Sommer, and K. Stahr. 2002. Linking soil classification and soil dynamics: Pedological and ecological perspectives. J. Plant Nutr. Soil Sci. 165:517–529. doi:10.1002/1522-2624(200208)165:4<517::AID-JPLN517>3.0.CO;2-#

Gannon, J.P. 2014. A hydropedological approach to describing runoff generation, lateral podzolization, and spatial and temporal patterns in DOC in a headwater catchment. Ph.D. diss. Virginia Polytechnic Inst. and State Univ., Blacksburg.

Jankowski, M. 2014. The evidence of lateral podzolization in sandy soils of northern Poland. Catena 112:139–147. doi:10.1016/j.catena.2013.03.013

Likens, G.E., and F.H. Bormann. 1995. Biogeochemistry of a forested ecosystem. 2nd ed. Springer-Verlag, New York.

Löfgren, S., and N. Cory. 2010. Groundwater Al dynamics in boreal hillslopes at three integrated monitoring sites along a sulphur deposition gradient in Sweden. J. Hydrol. 380:289–297. doi:10.1016/j.jhydrol.2009.11.004

Lucas, Y., C.R. Montes, S. Mounier, M. Loustau Cazalet, D. Ishida, R. Achard, et al. 2012. Biochemistry of an Amazonian podzol–ferralsol system with white kaolin. Biogeoscience 9:3705–3720. doi:10.5194/bg-9-3705-2012

Lundstrom, U.S., N. van Breemen, and D. Bain. 2000. The podzolization process: A review. Geoderma 94:91–107. doi:10.1016/S0016-7061(99)00036-1

McKeague, J.A., F. DeConinck, and D.P. Franzmeier. 1983. Spodosols. In: L.P. Wilding et al., editors, Pedogenesis and soil taxonomy: II. The soil orders. Elsevier, New York. p. 217–252.

McSweeney, K., and E.A. FitzPatrick. 1990. Microscopic characterization of the Spodic horizon. In: J.M. Kimble and R.D. Yeck, editors, Proceedings of the 5th International Soil Correlation Meeting (V-IS-COM): Characterization, Classification and Utilization of Spodosols. USDA Soil Conserv. Serv., Lincoln, NE. p. 211–220.

Schoeneberger, P.J., D.A. Wysocki, E.C. Benham, and Soil Survey Staff. 2012. Field book for describing and sampling soils, Version 3.0. Natl. Soil Surv. Ctr., Lincoln, NE.

Soil Survey Staff. 2004. Soil survey laboratory methods manual. Soil Surv. Invest. Rep. 42. Version 4.0. Natl. Soil Surv. Ctr., Lincoln, NE.

Soil Survey Staff. 2010. Keys to soil taxonomy. 11th ed. NRCS, Washington, DC.

Sommer, M., D. Halm, C. Geisinger, I. Andruschkewitsch, M. Zarei, and K. Stahr. 2001. Lateral podzolization in a sandstone catchment. Geoderma 103:231–247. doi:10.1016/S0016-7061(01)00018-0

Sommer, M., D. Halm, U. Weller, M. Zarei, and K. Stahr. 2000. Lateral podzolization in a granite landscape. Soil Sci. Soc. Am. J. 64:1434–1442. doi:10.2136/sssaj2000.6441434x

Sommer, M., and E. Schlichting. 1997. Archetypes of catenas in respect to matter: A concept for structuring and grouping catenas. Geoderma 76:1–33. doi:10.1016/S0016-7061(96)00095-X

Stoops, G. 2003. Guidelines for analysis and description of soil and regolith thin sections. SSSA, Madison, WI.

Teets, J., and G. Nowacki. 2012. Conservation and restoration of America's great outdoors: Soil science adds additional restoration tools. West Virginia NRCS News and Views, August. http://www.nrcs.usda.gov/Internet/FSE_DOCUMENTS/nrcs144p2_072125.pdf (accessed 2 Nov. 2014).

Thomas, G.W. 1986. Soil pH and soil acidity. In: D.L. Sparks, editor, Methods of soil analysis. Part 3. Chemical methods. SSSA Book Ser. 5. SSSA and ASA, Madison, WI. p. 475–490. doi:10.2136/sssabookser5.3.c16

Zimmer, M.A., S.W. Bailey, K.J. McGuire, and T.D. Bullen. 2013. Fine scale variations of surface water chemistry in an ephemeral to perennial drainage network. Hydrol. Processes 27:3438–3451. doi:10.1002/hyp.9449